JOURNAL OF SOLID STATE CHEMISTRY 107, 171–178 (1993)

Crystal Structure of Monoclinic $MnSe_2O_5$ and Comparative Magnetic Study of Monoclinic and Orthorhombic Varieties

J. BONVOISIN, J. GALY, AND J. C. TROMBE

Centre d'Elaboration des Matériaux et d'Etudes Structurales, Laboratoire d'Optique Electronique, CNRS, 29 rue Jeanne Marvig, BP 4347, 31055 Toulouse Cedex, France

Received November 16, 1992; in revised form March 22, 1993; accepted March 24, 1993

Manganese diselenite, $MnSe_2O_5$, exhibits two allotropic forms. The structure of the monoclinic *m* variety has been determined (a = 7.960(3), b = 10.938(1), c = 5.850(2)Å, β = 118.27(2)°, Z = 4, space group = $C2/c$) and compared with the structure orthorhombic one, *o*. Both structures present similarities: (1) zigzagging chains of octahedra [MnO_6], running along the [001] axis; (2) each octahedron shares opposite edges with the two neighbor ones; (3) Mn–Mn intrachain distances are similar, 3.4422(8) Å for the monoclinic vs 3.394(2) Å for the orthorhombic; (4) each chain is interconnected with six other chains via $Se_2O_5^{2-}$-anions. Differences appear between the *m* and *o* forms are also apparent: (1) the zigzagging angle is sharper in the former; (2) the bridge angle Se–O–Se is higher in the *m* form in comparison to other diselenites including the *o* form; (3) the interchain distances range from 5.169 Å to 7.965 Å for *m*, and between 6.190 Å to 6.822 Å for the *o* form. Differences are also noticed by infrared spectra. The phase transformation $m \Leftrightarrow o$ does not occur by heating, even up to decomposition. A magnetic study of both varieties shows a weak antiferromagnetic interaction between manganese ions along a chain and reveals the occurrence of a long range antiferromagnetic ordering at significantly different temperatures: T_N = 9 and 5.2 K for *m* and *o* species, respectively. A magnetostructural correlation is proposed.

Introduction

The structural chemistry of selenites is very dependent upon the lone pair on the selenium (IV). This lone pair can play a particular role in the antiferromagnetic interaction of these compounds (*1, 2*): indeed, in $CuSe_2O_5$, it has been shown that the Se lone pairs can promote the exchange interaction when they are well oriented. Moreover, the (Se_2O_5) group, as bridging ligand, presents an additional interest: because of its polyatomic nature, the ferromagnetic contribution to the exchange interaction J vanishes (*1*).

Selenites or diselenites of manganese at various oxidation states (II, III, IV) have been described previously (*3–8*). Manganese(II) diselenite $MnSe_2O_5$ deserves our interest:

—Bertaud reported such a phase to be monoclinic, space group $C2/c$ or Cc, with a = 7.951, b = 10.959, c = 5.892 Å, β = 118.0°, V = 452 Å^3, but the structure was not analyzed (3).

—Koskenlinna *et al.* gave a structural description of $MnSe_2O_5$ in an orthorhombic system, space group $Pbcm$, with a = 6.822(3), b = 10.636(4), c = 6.323(3) Å, V = 458 Å^3(4). This variety was found to be isostructural with $ZnSe_2O_5$ (*3, 9*).

The present investigation was undertaken in order to shed some light on the possible existence of these two varieties *m* or *o* of $MnSe_2O_5$. The structure of the *m* form is determined and compared with the *o* one. Investigations have also been carried out to see if one of these forms could exhibit a phase transition upon heating. Besides, a magnetic study of both varieties is presented.

0022-4596/93 $5.00

Experimental

• *Synthesis and Characterization*

Both varieties were prepared in accordance with the literature data (*3*, *8*):

—for the first variety, *m*, a mixture of manganous oxide and selenium dioxide (molar ratio $\frac{1}{2}$) was introduced in an outgassed sealed Pyrex tube, was heated to around 400°C for 72 hr and cooled down slowly (*3*). Some single crystals appeared in this synthesis.

—for the second variety, *o* (*4*, *8*), a solution of selenium dioxide (20 mmol) in 50 ml (50%) acetic acid was added to a solution of manganese(II) acetate (10 mmol) in 50 ml acetic acid maintained at 60°C. Precipitation occurred after a few minutes; the precipitate was filtered, washed with 50% acetic acid, ethanol and ether and air dried.

The two varieties are light pink. Chemical analyses were performed by the Laboratoire Central de Microanalyse du CNRS: $MnSe_2O_5$, calculated wt%, Mn = 18.76, Se = 53.92; Observed wt%, for *m*, Mn = 18.7, Se = 52.5; for *o*, Mn = 18.3, Se = 53.4, H < 0.20, C < 0.20.

The X-ray powder diffraction patterns of these two compounds, clearly different, may be indexed using the cell constants of the two varieties of $MnSe_2O_5$ (*3*, *4*). Differences are also reflected by the infrared spectra of these two compounds. Data

TABLE I

EXPERIMENTAL CRYSTALLOGRAPHIC DATA FOR MONOCLINIC $MnSe_2O_5$

	Crystal data		
Crystal system:	Monoclinic	Space group:	*C*2/*c*
a (Å)	= 7.960(3)		
b (Å)	= 10.938(1)	β	= 118.27(2)°
c (Å)	= 5.850(2)		
V (Å^3)	= 448.6(3)	*Z*	= 4
Molecular weight (g)	= 292.86	ρ_{cal} (g/cm^3))	= 4.34
μ (MoK_α) (cm^{-1})	= 185		
Morphology:	Parallelipiped	Dimension (mm)	= 0.5 × 0.1 × 0.1
Transmission coefficient:	min. = 64	max. = 100.0	
	Data collection		
Temperature (K)	= 293	Wavelength (Mo$K\alpha$)	= 0.71073 (Å)
Monochromator:	graphite		
Scan mode	= $\omega - 2\theta$	Max. Bragg angle (°)	= 30
Scan width (°)	= 0.90 + 0.35 tan θ	Take-off angle (°)	= 2.75
Scan speed[a]			
SIGPRE[a]	= 0.85	SIGMA[a]	= 0.018
VPRE (°/min)[a]	= 6.70	T_{max} (s)[a]	= 80
Intensity control reflections (every 5400 sec)		4 0 2/5 7 2/6 0 0	
Orientation control reflections (every 150 reflections)		6 0 0/0 14 0/2 12 2	
	Structural refinement:		
Reflections collected	= 760		
Reflections used	= 570 ($I > 3\sigma(I)$)		
Number of refined parameters	= 39		
Weighting w^{-1}	= $\sigma^2(F_0) + (0.001\ F_0)^2$		
$R = \Sigma\|\|F_o\| - \|F_c\|\|/\Sigma\|F_o\|$	= 0.029		
$R_w = [\Sigma_w(\|F_o\| - \|F_c\|)^2/\Sigma_w F_o^2]^{1/2}$	= 0.040		s = 1.13

[a] For definition of parameters see Ref. (*10*).

TABLE II

ATOMIC POSITIONS AND EQUIVALENT THERMAL PARAMETERS FOR MONOCLINIC $MnSe_2O_5$

Atom	x	y	z	B_{eq} (Å)^2
Se	0.35240(5)	0.14130(3)	0.37969(6)	0.69(2)
Mn	½	0.41705(7)	¼	0.73(3)
O(1)	0.1564(3)	0.0651(3)	0.1733(5)	0.9(1)
O(2)	0.3098(4)	0.2838(2)	0.2754(6)	1.2(1)
O(3)	½	0.0809(4)	¼	2.6(2)

Note. $B_{eq} = 8\pi^2/3$ trace u (u = diagonalized U matrix).

concerning this technique, as well as thermal analyses, are reported in the discussion.

• *Crystal Structure Determination*

A single crystal of the *m* variety was mounted on a CAD4 Enraf–Nonius diffractometer. The orientation matrix and accurate cell constants were derived from least-squares refinement of the setting angles of 25 reflections. Crystal data and conditions of intensity measurements are reported in Table I. The standard reflections showed no abnormal trend. The data were corrected for Lorentz and polarisation effects; absorption corrections (*11*) and secondary extinction were applied in the last cycles of refinement.

Structure determination was refined by applying full-matrix least-squares procedures on an Alliant VFX/80 computer using programs listed in Ref. (*12*). Throughout the refinements, the minimized functions were $\Sigma_w(|F_o| - |F_c|)^2$, where F_o and F_c are the observed and calculated structure factor amplitudes. Scattering factors and anomalous terms were taken from Cromer and Waber (*13*). The structure was refined using the centrosymmetric group. The heavy atoms, selenium and manganese, were localized by the Patterson technique, the other atoms by using the difference Fourier map. Two atoms occupied special positions on a twofold axis, Mn and O(3); the remaining atoms were in general positions. Convergence was reached at $R = 0.029$, $R_w = 0.040$ for 570 reflections $I > 3\sigma(I)$ and 39 variables (Table I). In the last cycle of refinement, the largest (variable shift) (e.s.d.) ratio was less than to 0.01. A final Fourier map did not show any significant residual features.

Final atomic coordinates and equivalent thermal parameters are given in Table II; selected interatomic distances and bond angles are listed in Table III.

• *Magnetic Measurements*

Magnetic susceptibility measurements was studied on powder samples of about 35 and 26 mg for *m* and *o* respectively in the temperature range 4.2–300 K with a Faraday-type magnetometer (this apparatus has already been described in detail by Gardner and Smith (*14*)). Magnetic in-

TABLE III

SELECTED INTERATOMIC DISTANCES (Å) AND BOND ANGLES (°) IN $MnSe_2O_5$

m-form		*o*-form	
Se–O(1)	1.674(2)	Se–O(1)^{i}	1.67(1)
Se–O(2)	1.649(2)	Se–O(2)^{ii}	1.64(1)
Se–O(3)	1.800(2)	Se–O(3)^{iii}	1.830(7)
O(1)–Se–O(2)	104.2(1)	O(1)^{i}–Se–O(2)^{ii}	102.9(6)
O(1)–Se–O(3)	94.9(1)	O(1)^{i}–Se–O(3)^{iii}	95.8(5)
O(2)–Se–O(3)	104.6(2)	O(2)^{ii}–Se–O(3)^{iii}	102.6(8)
Se–O(3)–Se^{i}	136.9(2)	Se^{iii}–O(3)–Se^{iv}	121.6(8)
Mn–O(1)^{ii}	2.190(3)	Mn–O(1)	2.18(1)
Mn–O(1)^{iii}	2.190(3)	Mn–O(1)^{v}	2.18(1)
Mn–O(1)^{iv}	2.215(3)	Mn–O(1)^{ii}	2.21(1)
Mn–O(1)^{v}	2.215(3)	Mn–O(1)^{vi}	2.21(1)
Mn–O(2)	2.158(3)	Mn–O(2)	2.21(1)
Mn–O(2)^{i}	2.158(3)	Mn–O(2)^{v}	2.21(1)
Mn^{ii}–O(1)–Mn^{vi}	102.78(9)	Mn–O(1)–Mn^{v}	101.4(5)
Mn–Mn^{vii}	3.4422(8)	Mn–Mn^{iii}	3.394(2)
Mn–Mn^{viii}	3.4422(8)	Mn–Mn^{v}	3.394(2)
Mn^{vii}–Mn–Mn^{viii}	116.37(4)	Mn^{iii}–Mn–Mn^{v}	137.4(2)

Note. Equivalent positions: (*m*-form) i = 1 − *x*, 1 + *y*, ½ − *z*; ii = ½ − *x*, ½ − *y*, −*z*; iii = ½ + *x*, ½ − *y*, ½ + *z*; iv = ½ + *x*, ½ + *y*, *z*; v = ½ − *x*, ½ + *y*, ½ − *z*; vi = *x* − ½, *y* − ½, *z*; vii = 1 − *x*, 1 − *y*, 1 − *z*; viii = 1 − *x*, 1 − *y*, *z*; (*o*-form) i = ½ − *x*, ½ − *y*, ½ + *z*; ii = *x*, 1 − *y*, ½ + *z*; iii = 1 − *x*, 1 − *y*, 1 − *z*; iv = *x*, 1 − *y*, *z* − ½; v = 1 − *x*, *y*, ½ − *z*; vi = 1 − *y*, 1 − *y*, − *z*.

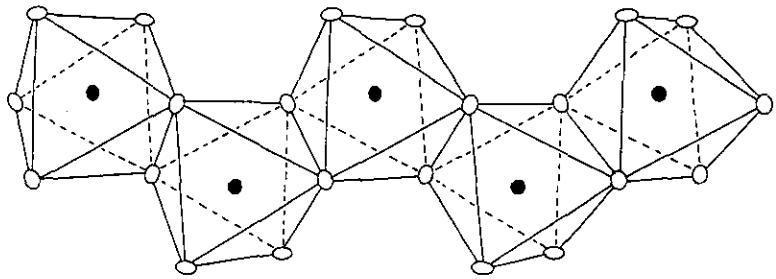

FIG. 1. View of the chains running along the [001] axis for the monoclinic variety: Mn = ●, O = ○.

duction of 1 T was used. Independence of the susceptibility from the magnetic induction was checked at both high and low temperatures. Mercuritetrathiocyanato cobaltate was used as a susceptibility standard. The diamagnetism was estimated as -102×10^{-6} cm^{3}mole^{-1}.

Results and Discussion

• *Description of the Monoclinic Structure in Comparison with the Orthorhombic One*

In spite of the discrepancy of their crystallographical systems, both varieties exhibit very similar structural packing. However, subtle differences appear in their respective structures.

For both structures, the manganese atom is surrounded by six oxygen atoms, leading to a slightly deformed octahedron presenting the C_2 site symmetry. The Mn–O distances are quite similar (Table III). Each octahedron shares an edge with the two neighbor octahedra to form zigzagging chains running along the *c* axis (Fig. 1). The Mn–Mn intrachain distances are equal to 3.4422(8) and to 3.394(2) Å for *m* and *o*, respectively. The zigzag chains are more bent in the former case with respective angles Mn–Mn–Mn 116.37(4)° vs 137.4(2)°, leading to Mn···Mn (second neighbor) values of the *c* parameters of 5.850(2) vs 6.323(3) Å.

Each chain is connected to six chains via $[Se_2O_5]$ groups. The interchain distances range from 5.169(1) to 7.960(3) Å for *m* vs 6.190 to 6.822 Å for *o*. For *m*, the diselenite anion presents bond lengths in agreement with the literature data (Table III). The distance Se–O(3) is rather small but not significantly so.

The high value for *m* of the bridge angle Se–O(3)–Se, 136.9(2)° versus 121.6(9)° for *o* is worthy of notice (*4*). This value deviates, by far, from the literature data: $ZnSe_2O_5$ (3,9), $VOSe_2O_5$ (*15*), $CuSe_2O_5$ (*16*), $(NH_4)_2Se_2O_5$ (*17*), $CoSe_2O_5$ (*18*). For these last compounds, this angle ranges from 119.6° to 122.9°. In manganese hydrogen selenite diselenite, $Mn(HSeO_3)(Se_2O_5)$, the angle Se–O–Se amounts to 126.4(4)°. The authors try to interpret the widening of this angle, with respect to the diselenites quoted above, as a consequence of short Se–O bonds in the bridge (1.781(8) and 1.801(8) Å) (*5*). As the Se–O bridge distances for *m* are similar to those reported for the previous compounds, the widening of this angle to 136.9° is so far inexplicable. The other angles around the selenium O–Se–O in *m* are compatible with those of such diselenite compounds (Table III). See Fig. 2 for a view of the monoclinic cell.

• *Infrared and Thermal Behavior*

In the light of structural information, it may be possible to account for the differences observed in the infrared data of both

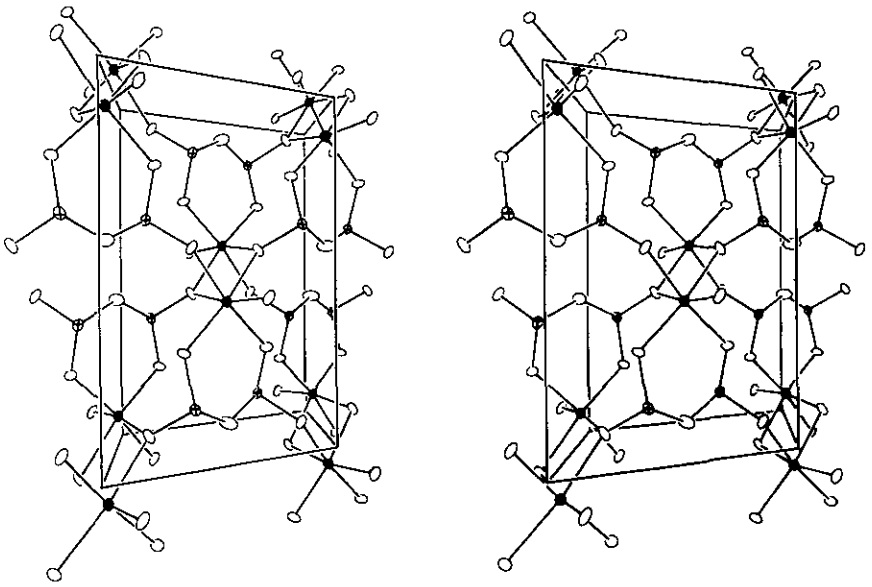

FIG. 2. Stereo view of the cell for the monoclinic variety along the c axis; where a = horizontal, b = vertical: Mn = ●, O = ○, Se = ⊕

varieties (Table IV). In these structures, the $Se_2O_5^{2-}$-anion presents a C_2 site symmetry. The bridge vibration Se–O–Se gives three bands around 510, 555, 585 cm^{-1} for o (*4*, *8*) and only one broad band localized at 622 cm^{-1} for m. This may be related chiefly to the modification of the bridge angle into the two structures. This phenomena also reaches the terminal vibrations (Table IV): the o infrared spectrum appears more split than the m one.

Differential thermal analysis (heating rate 5°/min) up to 400°C revealed no peaks that might indicate a possible transformation of these phases from one to the other: the X-ray diffraction powder patterns, after cooling, remain unchanged. Above 400°C, the thermogram of m looks like the thermogram of o previously described (*4*): evolution to $MnSeO_3$ between 400° and 435°C and decomposition of this latter phase to give Mn_2O_3 from 460° to 560°C.

If the o phase is heated to around 420°C in an outgassed Pyrex tube, in the presence of small amounts of SeO_2, the transformation into the m form is possible; otherwise nothing happens. The chemical analyses reported above are not in agreement with such an excess of SeO_2. This problem remains to be solved.

• *Magnetic Measurements*

The magnetic behavior of o and m is shown in Figs. 3a and b respectively in the form of plots of χ_M vs T.

Both varieties obey the Curie–Weiss law from 300 to 15 K, $1/\chi_M = (T - \Theta)/C$, with almost identical negative Curie–Weiss constants, $\Theta = -14.8$ K for o and $\Theta = -13.3$ K for m, suggesting a weak antiferromagnetic interaction between the Mn^{2+} ions. The Curie constants, $C = 4.63$ cm^3K mol^{-1} for m and $C = 4.73$ cm^3K mol^{-1} for o, are consistent with a spin $S = \frac{5}{2}$ with $g = 2$ ($C = Ng^2\beta^2S(S + 1)/3k = 4.38$ cm^3K mol^{-1}); the discrepancy is mainly due to the g factor, which is slightly different than 2.

Below 15 K, two main features to be pointed out are as follows:

(i) The susceptibility values are higher in o than in m at the same temperature. This should favor a smaller short-range antiferro-

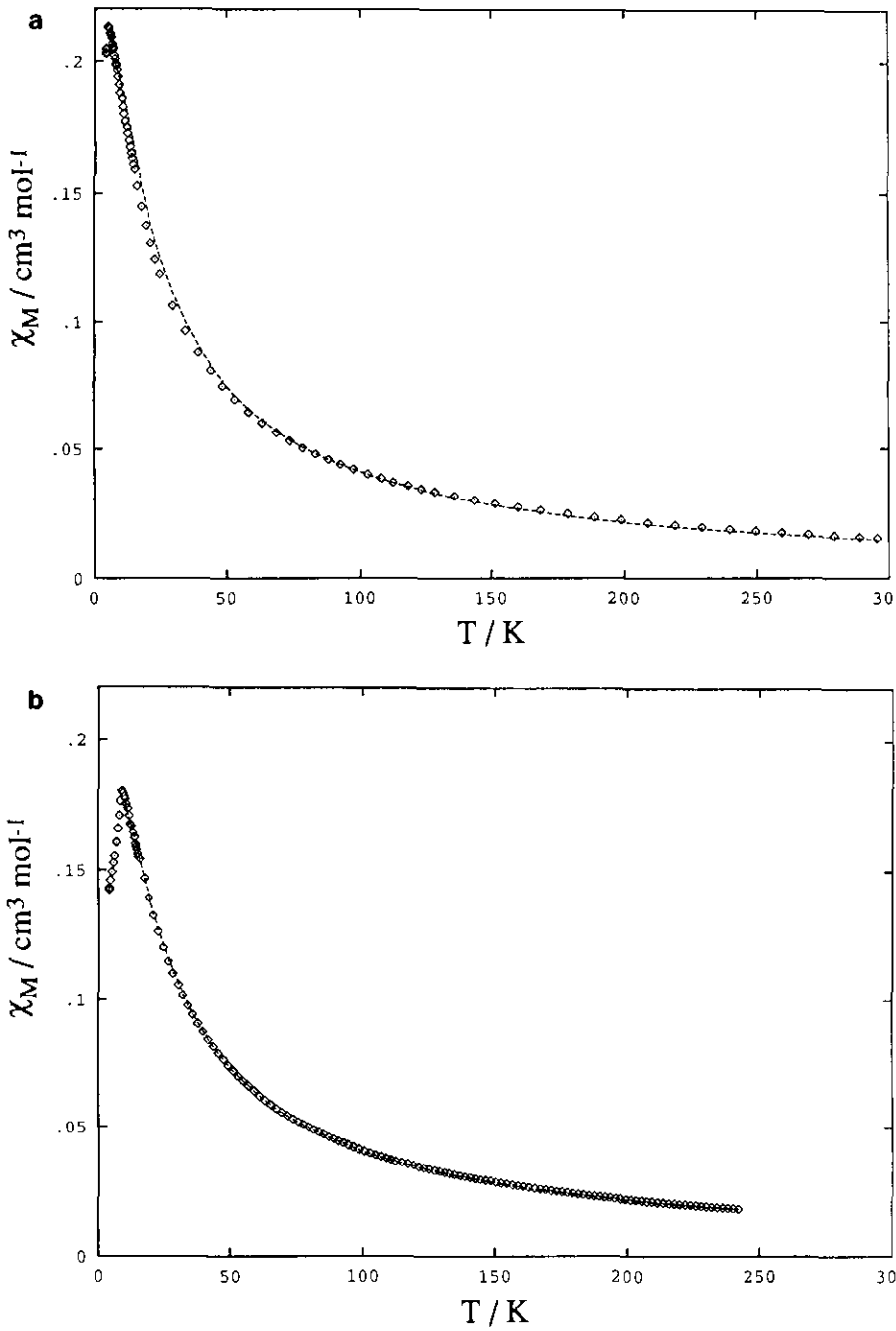

FIG. 3. Thermal variation of the molar susceptibility for $MnSe_2O_5$. (a) Orthorhombic species: Experimental points (◇); calculated points (– – –). (b) Monoclinic species: Experimental points (◇); calculated points (– – –).

TABLE IV

INFRARED ABSORPTION FREQUENCIES IN THE DOMAIN 1000–400 cm^{-1} OF $MnSe_2O_5$

Assignment	*o*-form x	*o*-form y	*m*-form
Se–O terminal	870 s	872 s	879 s
	845 m	850 s	858 sh
	830 m	836 s	783 vs
	760 vs,b	767 vs,b	
Se–O bridge	585 s	578 vs,b	
	555 vs		622 s,b
	510 m	519 m	
Se–O terminal	445 m	445 m	446 m
	410 w	420 sh	

Note. The letters mean: (x) frequencies observed in Ref. (2), (y) frequencies observed by us; s = strong, vs = very strong, m = medium, w = weak, b = broad, sh = shoulder.

magnetic coupling between manganese ions in the former case.

(ii) A drastic drop in χ_M may define the occurrence of a transition to a long range magnetic ordering at a critical temperature T_N which is different for the two species, $T_N = 5.2$ K for *o* and $T_N = 9$ K for *m*.

The magnetic data in the low dimensional regime may be fitted using Fischer's classical Heisenberg results for infinite linear chains. Fischer's equation for the magnetic susceptibility of a classical spin chain, scaled to a real spin, $S = \frac{5}{2}$, is (*19*, *20*)

$$\chi_{LC} = [Ng^2\beta^2S(S + 1)/3kT] \times \frac{(1 - u)}{(1 + u)}$$

where $u = -\coth K + 1/K$ and $K = JS(S + 1)/kT$, and the exchange Hamiltonian is written as $-JS_iS_j$ where J is the intrachain exchange parameter.

In the least-squares calculation, only the data above the ordering temperature have been taken into account and the agreement factor is defined as

$$R = [\Sigma(\chi_{obs} - \chi_{calc})^2/\Sigma\chi_{obs}^2]^{1/2}.$$

For *o*, the least-squares fits to the experimental data were attained using the parameters $g = 2.02$, $J = -1.06\ cm^{-1}$, and $R = 0.03$. A similar procedure was applied to *m* and the best fit parameters obtained were $g = 2.02$, $J = -1.18\ cm^{-1}$ and $R = 0.007$. The broken lines in Fig. 3 were generated with the parameters given above.

• *Discussion of Magnetic Results*

In general whatever the bridge is, it is usual to find weak magnetic interactions in manganese(II) chains; $MnCl_2 \cdot 2H_2O$ (*21*) $J = -0.31\ cm^{-1}$, $Mn(C_2O_4) \cdot 2H_2O$ (*22*) $J = -1.8\ cm^{-1}$, $Mn(C_{10}H_8N_2)(C_2O_4)$ (*23*) $J = -2.14\ cm^{-1}$ compared to other metallic chains, say copper(II) chains. This is usually explained by the fact that the exchange interaction decreases when the number of unpaired electrons increases on each site (*22*).

The intrachain exchange constants are almost equal in both compounds *o* and *m*; this is understandable because of the nearly identical Mn–Mn intrachain distance and Mn–O–Mn angles (cf. Table III).

Attempts to add an interchain exchange J' parameter by using molecular field approximation did not give any significant better fits. This is mainly due to the fact that no well "resolved" susceptibility maximum occurs above the transition temperature. This last fact brings about two points: (i) no accurate unique solution with J and J' can be found, so we preferred to keep the simplest model, which consists of a unique intrachain exchange parameter J; (ii) the interchain interaction may be of the same order of magnitude as the intrachain one as Kirk *et al.* pointed out (*24*).

Assuming the interchain interactions are not negligible, this allows us to explain why the transition temperature is higher in *m* than in *o*. The zigzag angle is sharper in *m* than in *o*, so the intrachain distance Mn–Mn (second neighbor) is also shorter. Moreover, the shortest interchain Mn–Mn distance occurs in *m*. All these facts should enhance the interchain interactions in *m* and promote the order transition at higher temperatures. The interactions would exist owing to the O–Se–O or O–Se–O–Se–O

bridges between the manganese ions. Extended Hückel calculation should provide a proof of this fact; we are working along this line.

Nevertheless, these results emphasize the importance of O–Se–O bridge pathways for exchange processes.

References

1. O. KAHN, M. VERDAGUER, J. J. GIRERD, J. GALY, AND F. MAURY, *Solid State Commun.* **34,** 971 (1980).
2. J. C. TROMBE, A. GLEIZES, J. GALY, J. P. RENARD, Y. JOURNAUX, AND M. VERDAGUER, *New J. Chem.* **11,** 321 (1987).
3. M. BERTAUD, Ph.D. Thesis, Bordeaux, FR (1974).
4. M. KOSKENLINNA, L. NUNISTO, AND J. VALKONEN, *Cryst. Struct. Commun.* **5,** 663 (1976); *Acta Chem. Scand. Ser. A* **30,** 836 (1976).
5. M. KOSKENLINNA AND J. VALKONEN, *Acta Chem. Scand. Ser A* **31,** 611 (1977); *Acta Chem. Scand. Ser. A* **31,** 638 (1977); *Acta Chem. Scand. Ser. A* **31,** 752 (1977).
6. G. GIESTER AND O. WILDNER, *J. Solid State Chem.* **91,** 370 (1991).
7. K. KOHN, K. INULLE, O. HORIE, AND S. I. AKIMOTO, *J. Solid State Chem.* **18,** 27 (1976).
8. K. A. R. SALIB, B. A. EL-SHETARY, AND S. L. STEFAN, *Indian J. Chem. Sect. A* **26,** 615 (1987).
9. G. MEUNIER AND M. BERTAUD, *Acta Crystallogr. Sect. B* **30,** 2840 (1974).
10. A. MOSSET, J. J. BONNET, AND J. GALY, *Acta Crystallogr. Sect. B* **33,** 2633 (1977).
11. N. WALKER AND D. STUART, *Acta Crystallogr. Sect. A* **39,** 158 (1983).
12. G. M. SHELDRICK, "SHELX 76" (program for crystal structure determination), University of Cambridge, Cambridge (1976); C. K. Johnson, ORTEP, Rep. ORNL-1974, Oak Ridge National Laboratory, Oak Ridge, TN (1965).
13. "International Tables for X-ray Crystallography," Vol. 4, Tables 2.2A and 3.3.1 Kynoch, Birmingham (1974).
14. W. E. GARDNER AND T. F. SMITH, *in* "Progress in Vacuum Microbalance Techniques" (T. Gast and E. Robens, Eds.), Vol. 1, p. 155, Heyden, London (1972).
15. G. MEUNIER, M. BERTAUD, AND J. GALY, *Acta Crystallogr. Sect. B* **30,** 2834 (1974).
16. G. MEUNIER, C. SVENSSON, AND A. CARPY, *Acta Crystallogr. Sect. B.* **32,** 2664 (1976).
17. S. CHOMNILPAN, *Acta Crystallogr. Sect. B* **36,** 675 (1980).
18. F. C. HAWTHORNE, L. A. GROAT, AND T. S. ERCIT, *Acta Crystallogr. Sect. C* **43,** 2042 (1987).
19. M. E. FISCHER, *Am. J. Phys.* **32,** 343 (1964).
20. G. R. WAGNER AND S. A. FRIEDBERG, *Phys. Lett.* **9,** 11 (1964).
21. J. N. MCELEARNEY, S. MERCHANT, AND R. L. CARLIN, *Inorg. Chem.* **12,** 906 (1973).
22. J. J. GIRERD, Ph.D. Thesis, Université de Paris-Sud, Orsay (1982).
23. S. MENAGE, Ph.D. Thesis, Université de Paris-Sud, Orsay (1988).
24. M. L. KIRK, M. S. LAH, C. RAPTOPOULOU, D. P. KESSISSOGLOU, W. E. HATFIELD, AND V. L. PECORARO, *Inorg. Chem.* **30,** 3900 (1991).